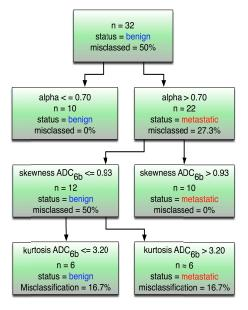
MULTI-SCALE ANALYSIS OF APPARENT DIFFUSION COEFFICIENT (ADC) PREDICTS CERVICAL NODAL STATUS IN PATIENTS WITH HEAD AND NECK SQUAMOUS CELL CARCINOMA

Shonit Punwani¹, Pierpaolo Purpura¹, Nikolaos Dikaios¹, Heather Fitzke¹, Alan Bainbridge², David Price², Scott Rice¹, Simon Morley³, Timothy Beale³, Ruheena Mendes⁴, Martin Forster⁴, Dawn Carnell⁴, Thayalini Vaitilingam³, Nina Newton¹, David Atkinson¹, Steve Halligan¹, and Stuart Taylor¹

¹Centre for Medical Imaging, University College London, London, UK, United Kingdom, ²Medical Physics and Bioengineering, University College London Hospital, London, United Kingdom, ³Radiology, University College London Hospital, London, United Kingdom, ⁴Head and Neck Oncology, University College London Hospital, London, United Kingdom

Introduction: Disease recurrence following therapy occurs in 50% of patients with head and neck squamous cell carcinoma (SCC) who present with nodal metastases at initial staging [1]. Accurate staging of nodal disease is pivotal for therapy selection and subsequent surveillance. Computed tomography (CT) and anatomical magnetic resonance imaging (MRI) have similar performance for detection of cervical nodal metastasis with a reported accuracy 78% and 82% respectively [2]. Diffusion weighted imaging (DWI) has been proposed as a 'functional' MRI technique to aid characterisation of cervical nodes [3]. However there is uncertainty whether ADC thresholds can be applied to discriminate benign from metastatic cervical nodes [4,5]. A number of methods are available to extract additional parameters from diffusion-weighted images; these may potentially aid discrimination of benign from metastatic nodes. Our aim was to assess multi-scale diffusion parameters (median volumetric nodal region of interest values, inter-voxel histogram distributions, and intra-voxel diffusion heterogeneity as assessed by the stretched exponential model) as classifiers of nodal status in patients with head and neck SCC.

Method: Patient Selection: Sixteen consecutive patients (mean age 61.8 years, 3 female) satisfying inclusion criteria of histologically confirmed head and neck SCC with unilateral cervical nodal (N2a/N2b/N3) metastatic disease were recruited prior to primary chemoradiotherapy, between March 2010 and June 2011. Patients with only unilateral metastatic disease were chosen for study inclusion so as to include benign contra-lateral nodes for subsequent comparison. All patients underwent contrast enhanced CT, routine MRI and neck ultrasound ± fine needle aspiration of lymph nodes to confirm nodal status. Diffusion Imaging Protocol: Axial diffusion weighted images of the neck were acquired supine using a 1.5T Siemens Avanto (Siemens, Erlangen, Germany) magnet with the manufacturer's carotid coils. A Short Tau Inversion Recovery - Echo Planar Imaging (STIR-EPI) sequence using diffusion gradients applied in 3 orthogonal directions at each of 6 b-values (0, 50, 100, 300, 600 and 1000s/mm²) was used. Trace diffusion-weighted images for each slice were automatically reconstructed using the manufacturers workstation (Siemens, Erlangen, Germany). ADC maps using all 6 bvalues (ADC_{6b}), low b-values alone (0, 50 and 100) (ADC_{fast}), and high b-values alone (300, 600 and 1000) (ADC_{slow}) were derived from the trace images by a mono-exponential non-linear least squares (Levenberg-Marquardt algorithm) fit performed using a commercial software package (MATLAB 2011b, The MathWorks Inc., Natick, MA, 2000). A further stretched exponential fit was performed using the same software, and α value and stretched exponential distributed diffusion coefficient (DDC) maps derived. Two experienced radiologists contoured the entire volume of solid components of the abnormal cervical node and separately the contralateral normal node on b300 images. ROIs from the b300 images were transferred electronically to corresponding parameter maps (ADC6b, ADCfast and ADC_{slow}, α value and DDC), and a list of voxel by voxel parameter values for metastatic and benign cervical nodes derived. Median



/ical nodal

values for the entire tissue volume for benign and metastatic nodes were calculated for each parametric map. The population distribution histogram of each parameter for benign and metastatic nodal volumes was plotted and skewness and kurtosis of the distributions recorded. *Statistical Analysis:* Histogram skewness, histogram kurtosis and median values of ADC_{6b}, ADC_{fast} and ADC_{slow}, α value and DDC were compared between benign and metastatic cervical nodes using the Wilcoxon matched pairs signed rank test using a commercial statistic package (Prism 5.0 for Mac, GraphPad Software, San Diego California USA). A multivariate decision tree analysis was performed using all parameters to derive a predictive model for classification of nodal status. A receiver operator characteristic (ROC) curve was generated for prediction of metastatic nodal status and the area under the curve (AUC) calculated.

Results: Median ADC_{fast} was lower in metastatic $(1.55 \times 10^{-3} \text{mm}^2/\text{s})$ than benign $(2.0 \times 10^{-3} \text{mm}^2/\text{s})$ nodes (p=0.007). There was no significant difference between benign and metastatic nodes for all other parameters (p=0.052 to 0.187). Intra-voxel ADC heterogeneity was greater in benign verses metastatic nodes (α value:0.68 and 0.76; p=0.002). Inter-voxel histogram distributions of ADC_{6b} (1.07 vs. 0.189; p=0.002) and ADC_{slow} were more positively skewed (1.08 vs. 0.162; p=0.002), and α (0.002 vs. 0.25; p=0.041) less positively skewed in metastatic nodes. There was no significant difference for histogram skewness or kurtosis between benign and metastatic nodes for any other derived parameter (p=0.074 to 0.979). The decision tree diagram for classification of benign and metastatic nodes is shown in figure 1. The median α value, skewness of ADC_{6b} histogram and the kurtosis of the ADC_{6b} histogram had a relative importance of 100%, 37.5% and 36.7% respectively. The ROC-AUC for the prediction of metastatic nodal status was 0.97.

^[1] Pryor et al. Asia Pac J Clin Oncol. 2011;7(3):236-51. [2] van den Brekel et al. Eur Arch Otorhinolaryngol. 1993;250(1):11-7. [3] Wang et al. Radiology. 2001;220(3):621-30. [4] Vandecaveye et al. Radiology. 2009;251(1):134-46. [5] Sumi et al. AJR Am J Roentgenol. 2006;186(3):749-57.